Title: Electrophysiological evidence that directional deep brain stimulation activates distinct neural circuits in patients with Parkinson's disease

Abbreviated title: Directional DBS activates distinct circuits

Authors and affiliations: Jana Peeters[a] MSc, Alexandra Boogers[a,b] MD, Tine van Bogaert[a] MSc, Hannah Davidoff[c] MSc, Robin Gransier[a] PhD, Jan Wouters[a] PhD, Bart Nuttin[d,e] MD PhD, Myles Mc Laughlin[a] PhD.

[a]Experimental Oto-rhino-laryngology, Department of Neurosciences, Leuven Brain Institute, KU Leuven, Herestraat 49, 3000 Leuven, Belgium

[b]Department of Neurology, UZ Leuven, Herestraat 49, 3000 Leuven, Belgium

[c]Animal and Human health engineering, Department of Biosystems, KU Leuven, Kasteelpark Arenberg 30, 3000 Leuven, Belgium

[d]Experimental Neurosurgery and Neuroanatomy, Department of Neurosciences, Leuven Brain Institute, KU Leuven, Herestraat 49, 3000 Leuven, Belgium

[e]Department of Neurosurgery, UZ Leuven, Herestraat 49, 3000 Leuven, Belgium

Corresponding author: Jana Peeters. Address: Herestraat 49, O&N 1, postal bus 721, 3000 Leuven, Belgium. Telephone: +32 16 377 848. E-mail: jana.peeters@kuleuven.be

Financial disclosures/Conflict of interest

J. Peeters' research was funded by Boston Scientific, VLAIO and EIT Health. A. Boogers' research was funded by Boston Scientific, VLAIO and EIT Health. T. Van Bogaert's research was funded by Boston Scientific, VLAIO and EIT Health. H. Davidoff reports no disclosures relevant to the manuscript. R. Gransier reports no disclosures relevant to the manuscript. J. Wouters reports no disclosures relevant to the manuscript. B. Nuttin has received grants from Medtronic and Boston Scientific. M. Mc Laughlin reports no disclosures relevant to the manuscript.

Abstract

Objectives: Deep brain stimulation (DBS) delivered via multi-contact leads implanted in the basal ganglia is an established therapy to treat Parkinson's disease (PD). However, the different neural circuits that can be modulated via stimulation on different DBS-contacts are poorly understood. Evidence shows that electrically stimulating the subthalamic nucleus (STN) causes a therapeutic effect via antidromic activation of the hyperdirect pathway - a monosynaptic connection from the cortex to the STN. Recent studies suggest that stimulating the substantia nigra pars reticulata (SNr) may improve gait. The advent of directional DBS leads now provides a spatially precise means to probe these neural circuits and better understand how DBS affects distinct neural networks.

Materials & Methods: We measured cortical evoked potentials (EPs) using electroencephalography (EEG) in response to low-frequency DBS using the different directional DBS-contacts in eight PD patients.

Results: A short-latency EP at 3ms originating from the primary motor cortex appeared largest in amplitude when stimulating DBS-contacts closest to the dorsolateral STN ($p < 0.001$). A long-latency EP at 10ms originating from the premotor cortex appeared strongest for DBS-contacts closest to SNr ($p < 0.0001$).

Conclusion: Our results show at the individual patient level that electrical stimulation of different nuclei produces distinct EP signatures. Our approach could be used to identify the functional location of each DBS-contact and thus help patient-specific DBS programming.

Key words: Movement disorders, Parkinson's disease, deep brain stimulation, electroencephalography, evoked potentials

Introduction

Deep brain stimulation (DBS) is a neuromodulation method in which an electrode array (i.e. DBS lead) is implanted in a target brain region to deliver electrical stimulation[1,2]. DBS is an established treatment for medication-refractory movement disorders such as Parkinson's disease (PD)[3–6]. The mechanisms through which DBS modulates local and distributed brain functions are not yet fully understood. Recent studies have postulated that antidromic activation of the motor cortex via a corticosubthalamic 'hyperdirect' pathway (HDP) plays an important role in mediating the DBS therapeutic effect. The existence of HDP has been shown in tractography studies[7,8]. Single cell recordings in both 6-OHDA lesioned rodents[9–11] and in the nonhuman primate MPTP model[12] have shown invasively that the motor cortex is antidromically activated during subthalamic nucleus (STN) DBS but not during globus pallidus internus (GPi) DBS, providing direct evidence for a therapeutic role for HDP stimulation. Furthermore, DBS activation of HDP has also been evaluated in PD patients through evoked potential (EP) recordings using electroencephalography (EEG)[13] and electrocorticography[14], with both studies suggesting STN-DBS does activate HDP antidromically, consistent with a latency of approximately 3ms considering the fiber thickness and conduction velocity of this pathway.

When DBS leads are implanted in the STN, stimulation on specific contacts can activate the substantia nigra pars reticulata (SNr). High-frequency SNr stimulation is known to cause side effects, such as mood disturbances[15–17]. Interestingly, some evidence suggests that low-frequency SNr stimulation may have a theraputic effect on gait disorders and axial symptoms. The effect of co-stimulation of STN and SNr has been shown to positively impact the number of freezing episodes[18], but also appeared to improve sleep disturbances[19] and the ability to initiate voluntary movements[20] in PD patients. Neurophysiological correlates of SNr-DBS have only been investigated in a limited amount of studies[21,22].

The current study investigated neurophysiological markers of STN- and SNr-DBS using directional leads. Research has already shown that directional stimulation can improve clinical outcomes[23–26]. We therefore opted to use directional leads as these provide a more precise means to investigate neurophysiological markers. More specifically, we measured EEG-based cortical EPs during low-

frequency (10 Hz) DBS on the different contacts from directional leads in PD patients. We systematically investigated the effects of stimulation intensity and anatomical electrical contact position (direction and depth) on the EP. We also investigated the relationship between EP amplitude and DBS-contact location obtained from imaging data and brain atlases. We found that dorsolateral STN-DBS was associated with a 3ms short-latency EP over the motor cortex, supporting the hypothesis that HDP activation delivers a therapeutic effect. In contrast, SNr-DBS was associated with a 10ms longer-latency EP over the pre-motor cortex, providing evidence that DBS in different structures activates distinct neural circuits.

Materials & Methods

Participants & surgery

The study was approved by the Ethics Committee Research UZ/KU Leuven (S62373) and registered on ClinicalTrials.gov (NCT04658641). All subjects received oral and written information and provided oral and written informed consent. The study was conducted in conformity with the Declaration of Helsinki, the Belgian law of May 7th 2004 on experiments on the human person and in agreement with Good Clinical Practice guidelines.

Subjects that met the 'UK PD Society Brain Bank Clinical Diagnostic Criteria' for the diagnosis of idiopathic PD, were included in the study. Directional leads (Vercise Cartesia®, Boston Scientific (BSC, Valencia, CA, USA)) were bilaterally implanted in the STN. These leads have eight DBS-contacts arranged in a 1-3-3-1 configuration, which means there are four depths and the middle two depths are segmented into three directions (numbering of left lead: C1-C8; numbering of right lead: C9-C16, where 'C' stands for 'Contact'). The surgical procedure was performed as standard-of-care using microrecording technique.

In total, eight PD patients were included in this study. Patients were asked to participate in the study at least 3 months after their implantation surgery. Some patients agreed to participate twice so we have data from both hemispheres in these patients. In other patients, only one hemisphere was tested. In total, ten hemispheres were tested. All patients were asked to refrain from taking their medication 12 hours prior to the experiment. Demographic data and stimulation parameters used during the experiment are summarized in Table 1.

DBS stimulation

Before determining the therapeutic window (TW), stimulation was turned off in both hemispheres. TW was defined with a monopolar cathodic pulse (return on the case) with pulse width of 60 µs and frequency of 130 Hz using their clinical DBS-contact configuration. In the tested hemisphere, the stimulation intensity was then slowly increased in steps of 0.5 mA until rigidity in the contralateral wrist

was alleviated. This amplitude was termed the bottom of therapeutic window (bTW). Next, the stimulation intensity was further increased until the patient reported a non-transient stimulation-induced side effect (e.g. diplopia, dyskinesia, etc.), here referred to as top of therapeutic window (tTW). All stimulation was well tolerated. One hemisphere was tested at a time, while stimulation of the other hemisphere was turned off. For each DBS-contact, three intensities were tested in a monopolar setting: subthreshold stimulation (0TW), bTW and tTW, where 0TW was set at 0.5mA. 0TW was used as a positive control, where only the stimulation-induced artifact and no significant neural response was expected. The same stimulation intensities (i.e. one value for 0TW, for bTW and for tTW) were used for all DBS-contacts in one hemisphere to enable a correct comparison of the EPs across DBS-contacts. In the first patient tested, an intermediate stimulation intensity between bTW and tTW was tested as well (iTW). At each amplitude tested, 50 seconds of EEG data were recorded (details below) using a standard cathodic pulse delivered at a frequency of 10 Hz. This yielded a total of 500 data epochs of 100ms duration. After testing each of the intensities on one DBS-contact, the protocol was repeated using a different contact in a random order. Each contact was tested, as well as the segmented contacts in ring mode.

EEG

EEG recordings were performed with a 64-channel ActiveTwo system (BioSemi, Amsterdam, the Netherlands) with a sample rate of 16384 Hz and a built-in low-pass filter with a cut-off frequency of 3200 Hz. EEG was recorded using active recording electrodes positioned according to internationally standardized 10-20 system[27] and referenced to the vertex EEG channel (Cz). One additional EEG channel was attached to the skin on top of the neurostimulator to record the stimulation pulse (EXG1) and served as a trigger to align EPs. Time zero was defined as the rising edge of the active pulse. Furthermore, two additional EEG channels were attached to the left and right mastoid to record the stimulation pulse at a cranial location (i.e. the stimulus artifact) with negligible neural responses (Left mastoid: EXG2; Right mastoid: EXG3). Voltage offsets of the recording electrodes remained between -30 and 30 mV during the study session. All EEG recordings were made in an electrically shielded sound

booth. To minimize tension in the muscles supporting the head, the patient remained seated in a comfortable chair that supported the head and neck. To reduce movement-induced artifacts, participants were asked to move as little as possible during the study session. The start of an epoch was defined as the rising edge of the stimulation pulse recorded on EXG1. EPs on each EEG channel were then calculated by averaging the epochs together.

Artifact reduction by template subtraction method

For each epoch, the zero was defined by subtracting the mean of a 1ms period just prior to stimulus onset. Then the epochs were averaged to get the averaged EP. Linear interpolation between 2.0ms pre-stimulus and 0.7ms post-stimulus (i.e. the beginning of the passive charge recovery phase) was used to remove the high-amplitude artifact caused by the stimulation pulse (see Fig. 1). The average EP was calculated for each EEG channel. The EXG2 and EXG3 channels were averaged together to create an artifact template channel. The template was windowed between 0.7 and 6.2ms post-stimulus (yielding 87 samples) as this encompassed the charge recovery artifact. The next step was to scale the template to fit the EP on each EEG channel. This was done by first calculating the relative error between the template and each EP [(template-EP)/template]. The scaling factor was calculated by the mean of the first 40 error samples of the error (where the artifact was largest) and then used to rescale the template to fit the EP. Finally, the scaled template was subtracted for each EP to yield the artifact-reduced EP. Two bandpass 2nd-order Butterworth filters were applied to these EPs. One was designed for evaluation of short-latency responses with a high-pass cutoff frequency of 150 Hz and low-pass cutoff frequency of 1000 Hz. The other filter was designed for evaluation of long-latency responses with a high-pass cutoff frequency of 1 Hz and low-pass cutoff frequency of 150 Hz.

Software and statistical analysis

All data processing and statistical analyses were done in MATLAB 2020b (Mathworks, Natick, MA, USA). A significance level of 5% was used in all tests. The amplitude and latency of the EP peaks were determined based on the maximum value within a fixed time frame (i.e. for P3: between 2 and 5ms, for

P10: between 8 and 15 ms). For further analysis, we extracted a peak at 3ms and one at 10ms in all EPs during all conditions. All analyses on short-latency peaks were performed on the EP recorded via the motor cortex EEG channel ipsilateral to stimulation (i.e. F3 for left hemisphere and F4 for right hemisphere). Analyses on long-latency responses were performed on the EP recorded via the prefrontal EEG channel ipsilateral to stimulation (i.e. AF7 for left hemisphere and AF8 for right hemisphere). Since we wanted to investigate if distinct EPs could be evoked when stimulating the different DBS-contacts, we first performed three sets of statistics at the individual hemispheric level. By central limit theorem, the individual EPs recorded were conform to Gaussian assumptions so parametric statistics were used[28]. Thus, we used a two-way ANOVA to evaluate if DBS 1) intensity, 2) direction and 3) depth had an effect on EP peak amplitude as measured in each individual hemisphere. Since each EP consisted of more that 400 epochs, enough data was available to perform robust statistics at the individual hemispheric level. To investigate a relationship between the distance from each DBS-contact to relevant anatomical regions, we grouped all tested hemispheres and used a linear mixed model with hemispheres as a random factor and the distance to the anatomy and peak amplitude as fixed factors. Postoperative lead reconstruction analysis was performed using the Lead-DBS (version 2.5.3, Berlin, Germany)[29,30] image processing pipeline. This allowed us to determine the specific lead position and orientation. This open-source software allows localization of implanted leads based on individual patient imaging data. This software was also used to calculate the distance between the center of each DBS-contact to the closest voxel of certain brain regions. For all hemispheres, we selected the Distal atlas[31] that segments 101 nuclei (e.g. the whole STN, STN subregions, SN, etc.). The software then automatically calculates the distance between the center of every DBS-contact to the closest voxel of all brain regions within the selected brain atlas.

Results

Characterization and suppression of stimulation-induced artifact

The electrical pulses delivered during DBS caused a large stimulation artifact in the EEG recording, which can mask short-latency neural responses. The full artifact consists of the active pulse, followed by a passive recharge phase, resulting in a total length of 6ms. Figure 1A shows the first twelve individual stimulation pulses before template subtraction and averaging (subject 1; DBS-contact 14, tTW). The artifact is an order of magnitude larger than the neural response. Figure panels 1B-E illustrate the effectiveness of the template subtraction method used to remove the stimulation artifact. After template subtraction, neural response peaks are clearly observable in both the long and short-latency EPs. To confirm that the short-latency peaks were actual neural responses and not residual artifact we performed EEG recordings in a phantom head implanted with a DBS electrode (Fig. 1F-G). As expected, no neural-like response peaks were visible in the phantom head after artifact-reduction, showing the effectiveness of the artifact reduction method.

Quantification of EPs in response to stimulation intensity, direction and depth

Figure 2 shows the short- (A) and long-latency (B) EPs in response to DBS on each individual contact in the right hemisphere of subject 1. The short-latency EPs were recorded from the motor cortex EEG electrode ipsilateral to stimulation in all patients (i.e. EEG electrode F3 for the left hemisphere and F4 for the right hemisphere). The long-latency EPs were recorded via the prefrontal EEG electrode ipsilateral to stimulation (i.e. EEG electrode AF7 for the left hemisphere and AF8 for the right hemisphere). As expected, stimulation at 0TW was too small to evoke an EP since we are below the TW threshold. Stimulation at bTW caused a small, but distinguishable EP with a short-latency peak at 3ms (P3) and a long-latency peak at 10ms (P10). These response peaks became more apparent when increasing the current at iTW and were strongest at tTW. Data from all tested hemispheres are shown in the supplementary results in a similar format (Figs. 2-2 to 2-10). The amplitude of P3 was strongest in the motor cortex ipsilateral of stimulation, while the amplitude of P10 was strongest in the prefrontal cortex ipsilateral of stimulation. To illustrate this, topographic heat maps of the peak amplitudes recorded for P3 and P10 are shown in supplementary figure 4-1. In general, the EP morphology was in

good agreement with previously reported data recorded in similar populations [13,14]. To investigate neurophysiological markers of STN- and SNr-DBS, we investigated if changing stimulation parameters (i.e., intensity, direction and depth) affected EP morphology.

Distinct EP amplitudes were observed when stimulating at different DBS intensities

Fig. 3A and B show the effect of increasing stimulation intensity on the amplitude (mean ± CI) of the P3 and P10 peaks respectively for subject 1 (right hemisphere). The DBS-contact that evoked the highest P3 and P10 amplitudes was used. Similar figures are shown for all subjects in supplementary results (Figs. 3-2 to 3-10). ANOVA indicated that the stimulation intensity significantly affected both P3 ($F_{(3,1596)}$ = 257.8; $p < 0.0001$) and P10 ($F_{(3,1596)}$ = 770.9; $p < 0.0001$). At the group level, stimulation intensity affected P3 amplitude in 7/10 hemispheres and P10 in 10/10 hemispheres (Table 2). No significant effect of DBS intensity on P3 amplitude was found for subject 2 (left hemisphere), subject 6 (left hemisphere) and subject 7 (right hemisphere). This means that DBS probably did not elicit a distinguishable P3 in this hemisphere. Therefore, P3 directional and depth analysis were not performed for these hemispheres.

Distinct EP amplitudes were observed when stimulating on different directional contacts

Figure 3C and 3D show the peak amplitude (mean ± CI) for the EPs evoked with the ventral and dorsal segmented DBS-contacts in subject 1 (right hemisphere) for P3 and P10, respectively. To test if the changing stimulation direction had a significant effect on EP amplitude, we performed separate ANOVAs for each of the two segmented lead depths and for each of the peak amplitudes P3 and P10. We found that the stimulation direction significantly affected P3 amplitude for both the dorsal ($F_{(2,1197)}$ = 58.3; $p < 0.0001$) and the ventral ($F_{(2,1197)}$: 61.0; $p < 0.0001$) segmented DBS-contacts. Furthermore, we found that stimulation direction significantly affected P10 amplitude for both the dorsal ($F_{(2,1197)}$ = 25.2; $p < 0.0001$) and the ventral ($F_{(2,1197)}$ = 35.3; $p < 0.0001$) segmented DBS-contacts. At the group level, stimulation direction had a significant effect on P3 in 4/7 tested hemispheres, and a significant effect on P10 in 8/10 hempispheres (Table 2). To evaluate if directional stimulation significantly differs from omnidirectional stimulation, we performed three t-tests: each comparing the EP amplitude

recorded while stimulating using one segmented DBS-contact to the EP amplitude recorded while stimulating the segmented contacts in ring mode for each level separately. Results from this analysis are found in the supplementary material (Tables 2-1 and 2-2).

Distinct EPs amplitudes were observed when stimulating on different depth contacts

To investigate if the depth at which DBS was delivered has an effect on the P3 and P10 amplitude, a third ANOVA analysis was performed. For this analysis, only omnidirectional stimulation recordings were used to remove any possible effect of directionality. Fig. 3E and 3F show the P3 and P10 amplitude (mean ± CI) for the four omnidirectional depths for subject 1 (right hemisphere), respectively. In this subject, it is clear that P3 is largest on the most dorsal contacts, while P10 shows the opposite pattern being largest on the most ventral contacts. For this subject ANOVA showed a significant effect of depths on both P3 ($F_{(3,1596)} = 358.0$; $p < 0.0001$) and P10 ($F_{(3,1596)} = 494.2$; $p < 0.0001$) amplitude. At the group level, we observed that the depth of stimulation significantly affected P3 amplitude in 7/7 hemispheres and P10 amplitude in 9/10 hemispheres (Table 2).

Correlation between EP amplitudes and imaging-derived lead and contact position

The aforementioned results show that EP amplitude clearly changes with both contact direction and depth. These patterns also appeared to be different for the P3 and P10 peaks with more dorsal contacts tending to give larger P3 amplitudes and more ventral contacts tending to give larger P10 amplitudes. This supports the idea that stimulation on different DBS-contacts preferentially modulates different nuclei, which in turn give rise to the different EP peaks. To further investigate this, we plotted the average P3 and P10 amplitudes from all tested hemispheres as a function of the distance of each DBS-contact to dorsolateral STN and to SNr, respectively (Fig. 4). An analysis of this data using a linear mixed model showed that P3 had the highest amplitude when one of the (single) contacts closest to dorsolateral STN was stimulated (Fig. 4A) ($t_{(54)} = -3.75$; $R^2 = 0.54$; $p = 0.0004$). P10 had the highest amplitude when one of the (single) contacts closest to SNr was stimulated (Fig. 4B) ($t_{(54)} = -6.64$; $R^2 = 0.57$; $p < 0.0001$). An example of the lead position in subject 4 (left hemisphere) where STN and SNr are visualized using Lead-DBS [29], is shown in Figure 4C. Note that the more ventral located contacts

are closer to the SNr (blue region), while the more dorsal located contacts are closer to the STN (orange region).

Discussion

We recorded multichannel EEG EPs in response to STN- and SNr-DBS at different stimulation intensities, on different directional contacts and at different depths in ten hemispheres of eight PD patients. We succesfully applied a template-matching artifact reduction method that enabled the analyses of short- and long-latency EPs in all hemispheres during all DBS conditions. The general morphology and peak timings of the EPs correspond with EPs in response to STN-DBS reported in the literature[14,32–35]. We extracted the amplitude of the P3 peak in the short-latency EP and the P10 peak in the long-latency EP and used these to investigate if the different DBS conditions had an effect on the EP amplitude.

Our results show that increasing DBS intensities resulted in larger amplitude P10 EPs in all hemispheres while only 7 out of the 10 (70%) hemispheres showed this for the P3 peak. This was probably due to the overall smaller P3 peak magnitude, compared to the P10, makes it more difficult to detect P3 from the background noise. In the hemispheres where no significant effect of intensity was found on P3 amplitude, no further analyses were performed. Next, we found that DBS, delivered at different directional contacts, produced significantly different P3 amplitudes in 4 out of 7 hemispheres. In the remaining 3 hemispheres, the imaging data suggests that the lead was positioned medially in STN (the lead was positioned in dorsolateral STN for the remaining hemispheres), resulting in similar P3 amplitudes in all three directions. This may be the reason why P3 amplitude was not affected by direction. For the long-latency responses, we found that DBS delivered on different directional contacts produced significantly different P10 amplitudes in 8 out of 10 hemispheres. In the remaining 2 hemispheres, we identified two factors that could explain why P10 amplitude was the same on all directional contacts: 1) In subject 3 (left hemisphere), the ventral tip of the lead did not reach SNr and stimulation amplitude was limited to 3.0mA. This resulted in overall lower P10 EPs evoked with DBS. 2) In subject 7 (right hemisphere), we visually observed a difference in P10 amplitude between the different directional DBS-contacts. However, this effect was not significant because of large variability between the epochs. For the effect of depth, we found that DBS delivered on different depths produced

significantly different P3 amplitudes in all 7 hemispheres and significantly different P10 amplitudes in 9 out of 10 hemispheres. Subject 7 (right hemisphere) showed no significant difference in long-latency amplitude when comparing different depths, because of large variability between the epochs. Taken as a whole, our results indicate that DBS at different directional and depth contacts resulted in distinct EP signatures that are measurable at the level of the individual hemisphere. Below we discuss what our results suggest about the origin of P3 and P10 peaks.

The linear mixed model indicated that P3 had the largest amplitude when stimulating on the contact closest to dorsolateral STN, suggesting that P3 was associated with STN modulation (Fig. 4). The short-latency EPs we recorded are in close agreement with previous studies reporting a short-latency EP around 3ms [14,32–34,36]. These studies suggest that the P3 peak is caused by nonsynaptic, antidromic activation of the hyperdirect pathway[14,32–34,36]. This pathway is a monosynaptic axonal connection conveying input from the frontal cortex to STN[14,37]. Another possibility is that the P3 peak is caused by activation within STN itself[36]. It is known that EEG-based evoked potential methods can detect both cortical and deep brain sources[38,39].

We also showed that DBS-contacts closer to SNr, which were the most ventral contacts, resulted in a larger P10 amplitude (Fig. 4). A number of previous studies also report an EP peak around 10ms[32,35,40] but do not present data on the origin of this peak. Thus, our study provides the first evidence that this peak may be caused by stimulation of the SNr. However, future studies connecting EP peaks to structural connectivity via diffusion MRI tractography are key to strengthen this hypothesis.

Overall, our results indicate that distinct EPs can be recorded from the scalp when stimulating from the different DBS-contacts, providing evidence that DBS on different contacts activates different neural circuits. Thus, EPs may serve as a neurophysiological marker of STN- and SNr-DBS. This knowledge can improve our current understanding of how DBS affects the neural network, but could also have clinical implications. For example, EPs may be used as a complementary approach to the use of imaging to guide DBS programming in individual patients. The use of EPs to predict the most optimal DBS-

contact has already been investigated using electrocorticography[14]. In this study, the effect of various DBS parameters was investigated by comparing peak amplitudes and latencies. Their data suggested that a peak around 3ms was predictive of the DBS-contact that resulted in the best clinical outcome. However, they did not use directional leads, which have now become the new standard in clinical practice. The study presented here, provides the first insights on how directionality can affect both short- and long-latency EP responses in Parkinson's disease patients. We furthermore provide electrophysiological evidence that stimulation in different directions significantly affects P3 and P10 amplitude, which means there is an electrophysiological indication as to why we should direct the stimulation field towards dorsolateral STN, which is in agreement with clinical studies[23–26].

Further work investigating the relationship between EP amplitudes and clinical outcomes is necessary to strengthen the hypothesis presented here, but the results from our study indicate that it may be possible to use P3 as a predictor for the contact which most preferentially activates the HDP and thus leads to the best theraputic effect. In cases where P3 is strongest on one DBS-contact, it seems logical to choose that contact as a starting point to begin patient programming. However this strategy has not been tested yet. In cases where P3 is equally strong on more than one DBS-contact, the physician could consider dividing the total current over those DBS-contacts, thus dividing the current proportionally to P3 strength. P10 could be a predictive factor for side effect-causing regions (SNr). There is some evidence that stimulation of SNr-DBS at a lower frequency may help in gait problems [18]. In these cases, P10 could provide a means to predict which DBS-contact may be optimal when low-frequency stimulation is recommended.Thus, we believe the use of EPs to guide programming could be complementary to image-based approaches[41].

There are some potential limitations to be noted in this study. The sample size is modest. However, it must be noted that DBS-programming and lead positioning both happen on a patient-specific level. In our study, all statistics on the effect of DBS parameter settings on EP peak amplitude were performed on an individual (hemisphere) level. Another potential limitation is that we were not able to sufficiently reduce the stimulation related artifact in the first 2ms of the EP. It may be that within this short period

some very early EPs are present. Other studies do indeed report EPs at 1ms[13,14,35]. EPs evoked this early after onset of the DBS pulse could be volume conducted from direct STN activation[42] as robust large amplitude potentials have also been reported in STN after a stimulation pulse was given[43]. Another explanation came from the study of Miocinovic et al.[14] stating that EPs around 1 to 1.5ms are consistent with the known corticospinal conduction velocity of 40m/s[32] and estimated distance of 6.0cm between the motor cortex and the internal capsule. However, there is evidence from animal studies indicating that EPs around 1ms may be attributed to hyperdirect axon activation. Kumarvelu et al.[44] investigated the neural origin of STN DBS by recording cortical EPs in the parkinsonian rat brain and used a model of the thalamocrotical network to deconstruct the neural origin of the recorded EPs. They reported a peak around 1ms. When taking into account the size of the rat head and the distance between STN and the motor cortex (approximately 5mm) in rats, they estimate the conduction velocity of the hyperdirect axons to be around 5m/s. Furthermore, there are hyperdirect pathway axon tracing studies in rats[45] and in monkeys[46], where they injected a tracer in the motor cortex. These studies both report a hyperdirect pathway connecting the motor cortex to STN, amongst other brain structures, on the single-axon level.

In summary, we found that distinct EPs can be recorded from different DBS-contacts, depending on the direction and the depth of the DBS-contact and that these results are highly individualized. Furthermore, we found that P3 was strongly correlated to the distance of the DBS-contact to dorsolateral STN, while P10 was correlated to the distance of the DBS-contact to SNr. These results provide a strong indication that EPs may provide information on the location of an electrical contact, which could complement imaging data, and possibly help programming parkinsonian patients who received implants in STN.

Bibliography

1. Benabid AL, Pollak P, Gervason C, et al. Long-term suppression of tremor by chronic stimulation of the ventral intermediate thalamic nucleus. *Lancet*. 1991;337(8738):403-406. doi:10.1016/0140-6736(91)91175-t

2. Chiken S, Nambu A. Mechanism of Deep Brain Stimulation: Inhibition, Excitation, or Disruption? *Neurosci*. 2016;22(3):313. doi:10.1177/1073858415581986

3. Limousin P, Krack P, Pollak P, et al. Electrical Stimulation of the Subthalamic Nucleus in Advanced Parkinson's Disease. *N Engl J Med*. 1998;339(16):1105. doi:10.1056/NEJM199810153391603

4. Lyons MK. Deep brain stimulation: current and future clinical applications. *Mayo Clin Proc*. 2011;86(7):662-672. doi:10.4065/mcp.2011.0045

5. Kalia SK, Sankar T, Lozano AM. Deep brain stimulation for Parkinson,s disease and other movement disorders. *Curr Opin Neurol*. 2013. doi:10.1097/WCO.0b013e3283632d08

6. Fasano A, Bove F, Lang AE. The treatment of dystonic tremor: A systematic review. *J Neurol Neurosurg Psychiatry*. 2014. doi:10.1136/jnnp-2013-305532

7. Petersen M V, Lund TE, Sunde N, et al. Probabilistic versus deterministic tractography for delineation of the cortico-subthalamic hyperdirect pathway in patients with Parkinson disease selected for deep brain stimulation. *J Neurosurg*. 2017. doi:10.3171/2016.4.JNS1624

8. Chen Y, Ge S, Li Y, et al. Role of the Cortico-Subthalamic Hyperdirect Pathway in Deep Brain Stimulation for the Treatment of Parkinson Disease: A Diffusion Tensor Imaging Study. *World Neurosurg*. 2018;114:e1079-e1085. doi:10.1016/j.wneu.2018.03.149

9. Gradinaru V, Mogri M, Thompson KR, Henderson JM, Deisseroth K. Optical deconstruction of parkinsonian neural circuitry. *Science (80-).* 2009. doi:10.1126/science.1167093

10. Li Q, Ke Y, Chan DCW, et al. Therapeutic Deep Brain Stimulation in Parkinsonian Rats Directly Influences Motor Cortex. *Neuron*. 2012;76(5):1030-1041. doi:10.1016/j.neuron.2012.09.032

11. Sanders TH, Jaeger D. Optogenetic stimulation of cortico-subthalamic projections is sufficient to ameliorate bradykinesia in 6-ohda lesioned mice. *Neurobiol Dis*. 2016;95:225-237. doi:10.1016/j.nbd.2016.07.021

12. Johnson LA, Wang J, Nebeck SD, Zhang J, Johnson MD, Vitek JL. Direct activation of primary motor cortex during subthalamic but not pallidal deep brain stimulation. *J Neurosci*. 2020;40(10):2166-2177. doi:10.1523/JNEUROSCI.2480-19.2020

13. Walker HC, Huang H, Gonzalez CL, et al. Short latency activation of cortex during clinically effective subthalamic deep brain stimulation for Parkinson's disease. *Mov Disord*. 2012. doi:10.1002/mds.25025

14. Miocinovic S, de Hemptinne C, Chen W, et al. Cortical potentials evoked by subthalamic stimulation demonstrate a short latency hyperdirect pathway in humans. *J Neurosci*. 2018. doi:10.1523/JNEUROSCI.1327-18.2018

15. Bejjani B-P, Damier P, Arnulf I, et al. Transient Acute Depression Induced by High-Frequency Deep-Brain Stimulation. *N Engl J Med*. 1999;340(19):1476-1480. doi:10.1056/nejm199905133401905

16. Ulla M, Thobois S, Lemaire J-J, et al. Manic behaviour induced by deep-brain stimulation in Parkinson's disease: evidence of substantia nigra implication? *J Neurol Neurosurg Psychiatry*. 2006;77:1363-1366. doi:10.1136/jnnp.2006.096628

17. Blomstedt P, Hariz MI, Lees A, et al. Acute severe depression induced by intraoperative stimulation of the substantia nigra: A case report. *Park Relat Disord*. 2008;14(3):253-256. doi:10.1016/j.parkreldis.2007.04.005

18. Valldeoriola F, Muñoz E, Rumià J, et al. Simultaneous low-frequency deep brain stimulation of the substantia nigra pars reticulata and high-frequency stimulation of the subthalamic nucleus to treat levodopa unresponsive freezing of gait in Parkinson's disease: A pilot study. *Park Relat Disord*. 2019.

doi:10.1016/j.parkreldis.2018.09.008

19. Hidding U, Gulberti A, Pflug C, et al. Modulation of specific components of sleep disturbances by simultaneous subthalamic and nigral stimulation in Parkinson's disease. *Park Relat Disord*. 2019;62:141-147. doi:10.1016/j.parkreldis.2018.12.026

20. Heilbronn M, Scholten M, Schlenstedt C, et al. Anticipatory postural adjustments are modulated by substantia nigra stimulation in people with Parkinson's disease and freezing of gait. *Park Relat Disord*. 2019;66:34-39. doi:10.1016/j.parkreldis.2019.06.023

21. Galati S, Mazzone P, Fedele E, et al. Biochemical and electrophysiological changes of substantia nigra pars reticulata driven by subthalamic stimulation in patients with Parkinson's disease. *Eur J Neurosci*. 2006;23(11):2923-2928. doi:10.1111/J.1460-9568.2006.04816.X

22. McEvoy J, Ughratdar I, Schwarz S, Basu S. Electrophysiological validation of STN-SNr boundary depicted by susceptibility-weighted MRI. *Acta Neurochir (Wien)*. 2015;157(12):2129-2134. doi:10.1007/S00701-015-2615-1

23. Pollo C, Kaelin-Lang A, Oertel MF, et al. Directional deep brain stimulation: An intraoperative double-blind pilot study. *Brain*. 2014. doi:10.1093/brain/awu102

24. Steigerwald F, Müller L, Johannes S, Matthies C, Volkmann J. Directional deep brain stimulation of the subthalamic nucleus: A pilot study using a novel neurostimulation device. *Mov Disord*. 2016. doi:10.1002/mds.26669

25. Dembek TA, Reker P, Visser-Vandewalle V, et al. Directional DBS increases side-effect thresholds—A prospective, double-blind trial. *Mov Disord*. 2017. doi:10.1002/mds.27093

26. Krack P, Volkmann J, Tinkhauser G, Deuschl G. Deep Brain Stimulation in Movement Disorders: From Experimental Surgery to Evidence-Based Therapy. *Mov Disord*. 2019. doi:10.1002/mds.27860

27. Jasper H. The ten twenty electrode system of the international federation. *Electroencephalogr Clin Neurophysiol*. 1958.

28. Central Limit Theorem. In: *The Concise Encyclopedia of Statistics*. ; 2008. doi:10.1007/978-0-387-32833-1_50

29. Horn A, Kühn AA. Lead-DBS: A toolbox for deep brain stimulation electrode localizations and visualizations. *Neuroimage*. 2015. doi:10.1016/j.neuroimage.2014.12.002

30. Horn A, Li N, Dembek TA, et al. Lead-DBS v2 : Towards a comprehensive pipeline for deep brain stimulation imaging Region of Interest. *Neuroimage*. 2019;184(August 2018):293-316. doi:10.1016/j.neuroimage.2018.08.068

31. Ewert S, Plettig P, Li N, et al. Toward defining deep brain stimulation targets in MNI space: A subcortical atlas based on multimodal MRI, histology and structural connectivity. *Neuroimage*. 2018;170:271-282. doi:10.1016/J.NEUROIMAGE.2017.05.015

32. Ashby P, Paradiso G, Saint-Cyr JA, Chen R, Lang AE, Lozano AM. Potentials recorded at the scalp by stimulation near the human subthalamic nucleus. *Clin Neurophysiol*. 2001. doi:10.1016/S1388-2457(00)00532-0

33. Baker KB, Montgomery EB, Rezai AR, Burgess R, Lüders HO. Subthalamic nucleus deep brain stimulus evoked potentials: Physiological and therapeutic implications. *Mov Disord*. 2002. doi:10.1002/mds.10206

34. Kuriakose R, Saha U, Castillo G, et al. The nature and time course of cortical activation following subthalamic stimulation in parkinson's disease. *Cereb Cortex*. 2010. doi:10.1093/cercor/bhp269

35. Hartmann CJ, Hirschmann J, Vesper J, Wojtecki L, Butz M, Schnitzler A. Distinct cortical responses evoked by electrical stimulation of the thalamic ventral intermediate nucleus and of the subthalamic nucleus. *NeuroImage Clin*. 2018. doi:10.1016/j.nicl.2018.11.001

36. Schmidt SL, Brocker DT, Swan BD, Turner DA, Grill WM. Evoked potentials reveal neural circuits engaged by human deep brain stimulation. *Brain Stimul*. 2020. doi:10.1016/j.brs.2020.09.028

37. Nambu A, Tokuno H, Takada M. Functional significance of the cortico-subthalamo-pallidal "hyperdirect"

pathway. *Neurosci Res*. 2002. doi:10.1016/S0168-0102(02)00027-5

38. Gransier R, Hofmann M, van Wieringen A, Wouters J. Stimulus-evoked phase-locked activity along the human auditory pathway strongly varies across individuals. *Sci Rep*. 2021;11(1):143. doi:10.1038/s41598-020-80229-w

39. Gransier R, Guérit F, Carlyon RP, Wouters J. Frequency following responses and rate change complexes in cochlear implant users. *Hear Res*. 2021;404:108200. doi:10.1016/j.heares.2021.108200

40. Kelley R, Flouty O, Emmons EB, et al. A human prefrontal-subthalamic circuit for cognitive control. *Brain*. 2018. doi:10.1093/brain/awx300

41. Pavese N, Tai YF, Yousif N, Nandi D, Bain PG. Traditional Trial and Error versus Neuroanatomic 3-Dimensional Image Software-Assisted Deep Brain Stimulation Programming in Patients with Parkinson Disease. *World Neurosurg*. 2020;134:e98-e102. doi:10.1016/J.WNEU.2019.09.106

42. Maling N, Lempka SF, Blumenfeld Z, Bronte-Stewart H, McIntyre CC. Biophysical basis of subthalamic local field potentials recorded from deep brain stimulation electrodes. *J Neurophysiol*. 2018. doi:10.1152/jn.00067.2018

43. Sinclair NC, McDermott HJ, Bulluss KJ, et al. Subthalamic nucleus deep brain stimulation evokes resonant neural activity. *Ann Neurol*. 2018. doi:10.1002/ana.25234

44. Kumaravelu K, Oza CS, Behrend CE, Grill WM. Neural Circuits: Model-based deconstruction of cortical evoked potentials generated by subthalamic nucleus deep brain stimulation. *J Neurophysiol*. 2018;120(2):662. doi:10.1152/JN.00862.2017

45. Kita T, Kita H. The Subthalamic Nucleus Is One of Multiple Innervation Sites for Long-Range Corticofugal Axons: A Single-Axon Tracing Study in the Rat. 2012. doi:10.1523/JNEUROSCI.5717-11.2012

46. Coudé D, Parent A, Parent M. Single-axon tracing of the corticosubthalamic hyperdirect pathway in primates. *Brain Struct Funct*. 2018;223(9):3959-3973. doi:10.1007/S00429-018-1726-X

Table 1: Demographic data & Stimulation parameters

Subject No.	Gender	Age (yrs)	Therapeutic window (TW) determination			
			0TW (mA)	bTW (mA)	iTW (mA)	tTW(mA)
1R	F	**50**	0.5	2.0	4.0	6.0
1L	F	**50**	0.5	2.0		4.0
2L	M	**55**	0.5	2.5		5.0
3L	F	**58**	0.5	1.5		3.0
4L	F	**56**	0.5	2.0		4.0
5L	M	71	0.5	2.0		4.0
6L	M	47	0.5	3.0		6.0
7R	F	68	0.5	3.0		6.0
7L	F	68	0.5	3.0		6.0
8R	M	41	0.5	3.0		6.0
Average	4F/4M	55.8	0.5	2.4	4.0	5.0

***Legend**: L: left hemisphere tested; R: right hemisphere tested; 0TW: below bottom of therapeutic window; bTW: bottom of therapeutic window; iTW: between bottom and top of therapeutic window; tTW: top of therapeutic window*

Table 2: Effect of different stimulation intensities, direction and depth on P3 and P10 amplitude

Subject No.	Intensity P-value (F-statistics)		Directionality				Depth P-value (F-statistics)	
			Dorsal DBS-contacts P-value (F-statistics)		Ventral DBS-contacts P-value (F-statistics)			
	P3	P10	P3	P10	P3	P10	P3	P10
1R	< 0.0001 (257.8)	< 0.0001 (770.9)	< 0.0001 (58.3)	< 0.0001 (25.2)	< 0.0001 (61.0)	< 0.0001 (35.3)	< 0.0001 (358.0)	< 0.0001 (494.2)
1L	< 0.0001 (22.2)	< 0.0001 (862.2)	< 0.0001 (14.1)	< 0.0001 (45.7)	NS (0.34)	NS (1.9)	< 0.0001 (79.2)	< 0.0001 (301.0)
3L	0.0184 (4.0)	0.0268 (3.6)	NS (0.7)	NS (0.7)	NS (0.1)	NS (0.7)	< 0.0001 (9.2)	0.0407 (2.8)
4L	0.0147 (4.2)	< 0.0001 (285.5)	NS (2.3)	0.0489 (3.0)	NS (2.2)	NS (0.3)	< 0.0001 (69.7)	< 0.0001 (133.6)
5L	0.0002 (8.6)	< 0.0001 (11.8)	NS (0.9)	< 0.0001 (12.2)	NS (0.1)	NS (0.9)	0.0148 (3.5)	0.0226 (3.2)
7L	< 0.0001 (22.7)	< 0.0001 (143.5)	< 0.0001 (32.9)	< 0.0001 (25.0)	0.0005 (7.7)	< 0.0001 (13.7)	< 0.0001 (12.5)	< 0.0001 (45.4)
8R	< 0.0001 (35.9)	< 0.0001 (123.4)	0.0003 (8.2)	< 0.0001 (20.2)	NS (2.5)	< 0.0001 (45.7)	< 0.0001 (24.0)	< 0.0001 (36.4)
2L	NS (1.48)	< 0.0001 (34.5)	-	0.0027 (6.0)	-	NS (1.1)	-	< 0.0001 (7.2)
6L	NS (0.12)	< 0.0001 (267.1)	-	< 0.0001 (30.5)	-	0.0089 (4.7)	-	< 0.0001 (177.4)
7R	NS (0.4)	0.0419 (3.2)	-	NS (0.6)	-	NS (0.1)	-	NS (1.1)
Total (%)	7/10 (70%)	10/10 (100%)	4/7 (57%)	8/10 (80%)	2/7 (29%)	4/10 (40%)	7/7 (100%)	9/10 (90%)

Legend: *R: right hemisphere tested, L: left hemisphere tested*

Figure 1: Stimulation-induced artifact and reduction method

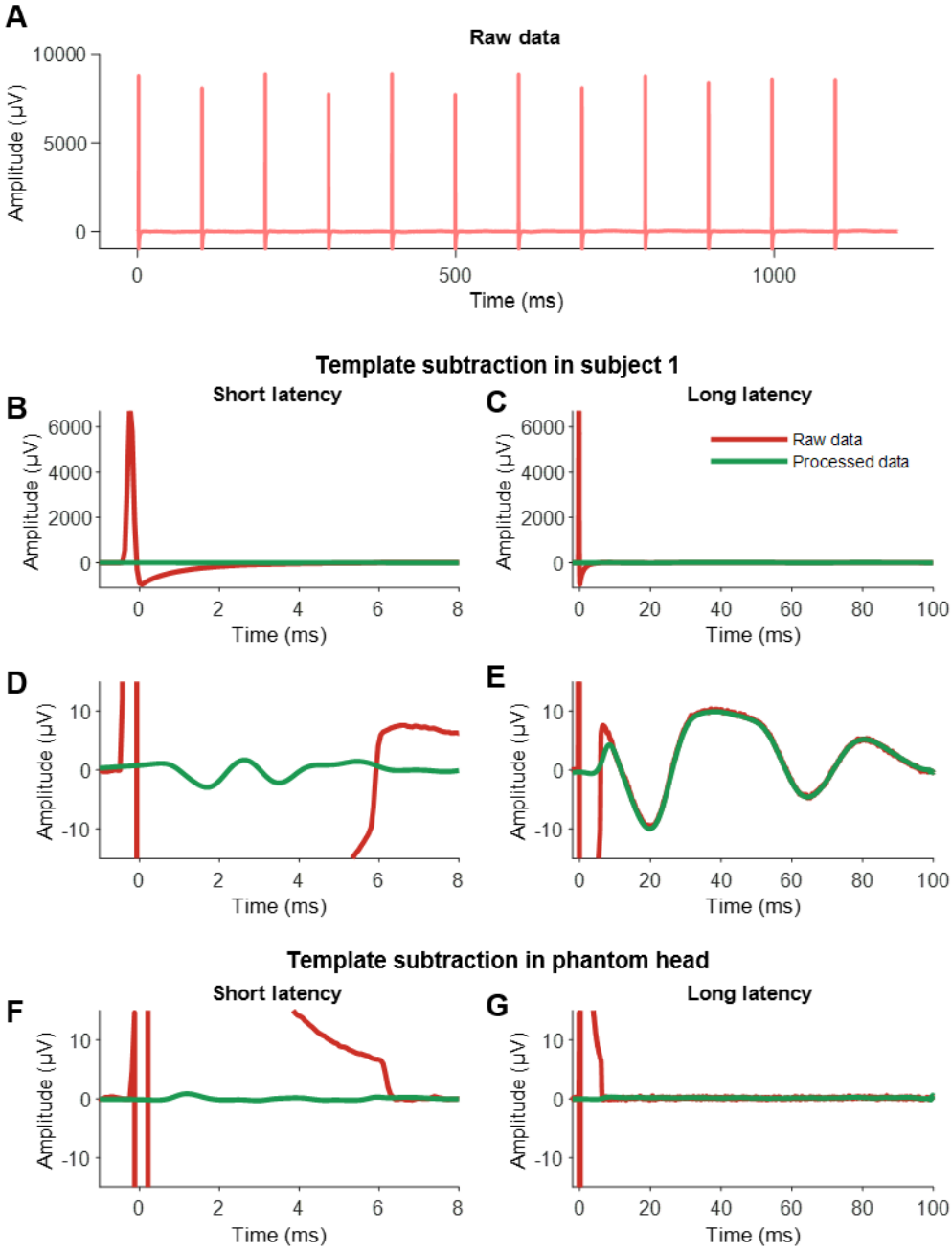

A) First 12 epochs (out of approximately 500) of the EP to STN stimulation. Each epoch has a duration of 100ms. B-E) A step-by-step visualization of the artifact-reduction method. The left panels (B and D) show the short-latency responses up to 8 ms, the right panels (C and E) show long-latency responses up to 100 ms. The lower panels show the same data but zoomed into to show the neural responses in the microvolt range. The red lines show the raw data prior to artifact reduction. The green lines show the processed data, after template subtraction and filtering. F-G) A visualization of the artifact reduction method in a phantom head. As expected no peaks (i.e. neural response) are apparent after artifact reduction.

Figure 2: Short- and long-latency EP responses – subject 1 (right hemisphere)

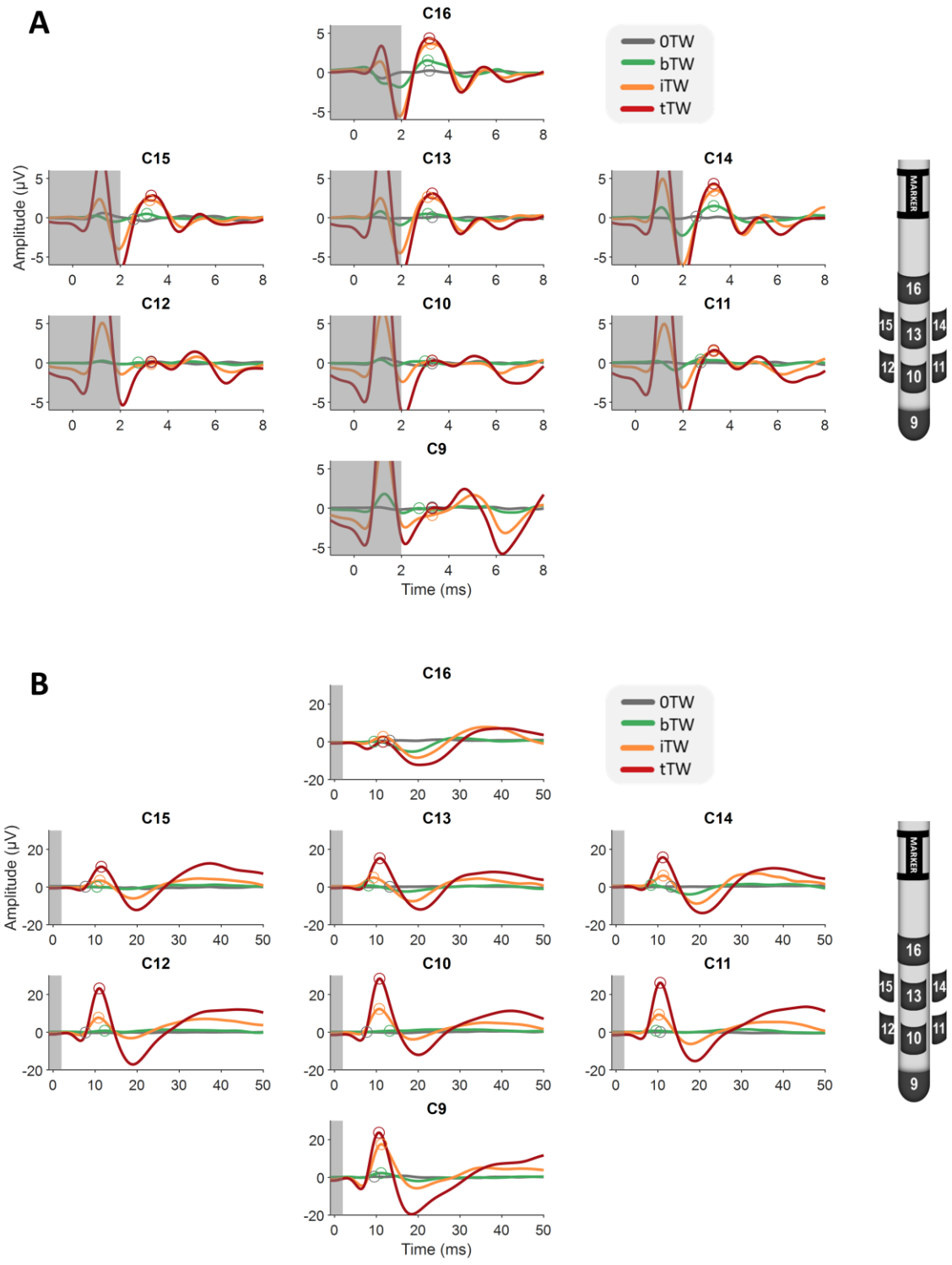

Short- (A) and long-latency (B) EPs. Each panel shows data from one DBS-contacts (shown on the right). Different colors show the EP in response to a different DBS intensities, where grey is subthreshold stimulation (0TW), green is bottom of the therapeutic window (bTW), orange is an intermediate intensity (iTW) and red is the top of the therapeutic window (tTW). The grey transparent box indicates the time window (-1 to 2ms) where residual artifact might still be present. No analyses were performed within this period window. The peaks are indicated with a circle for P3 and P10.

Figure 3: Effect of DBS intensity, direction and depth on the P3 and P10 peak amplitudes – subject 1 (right hemisphere)

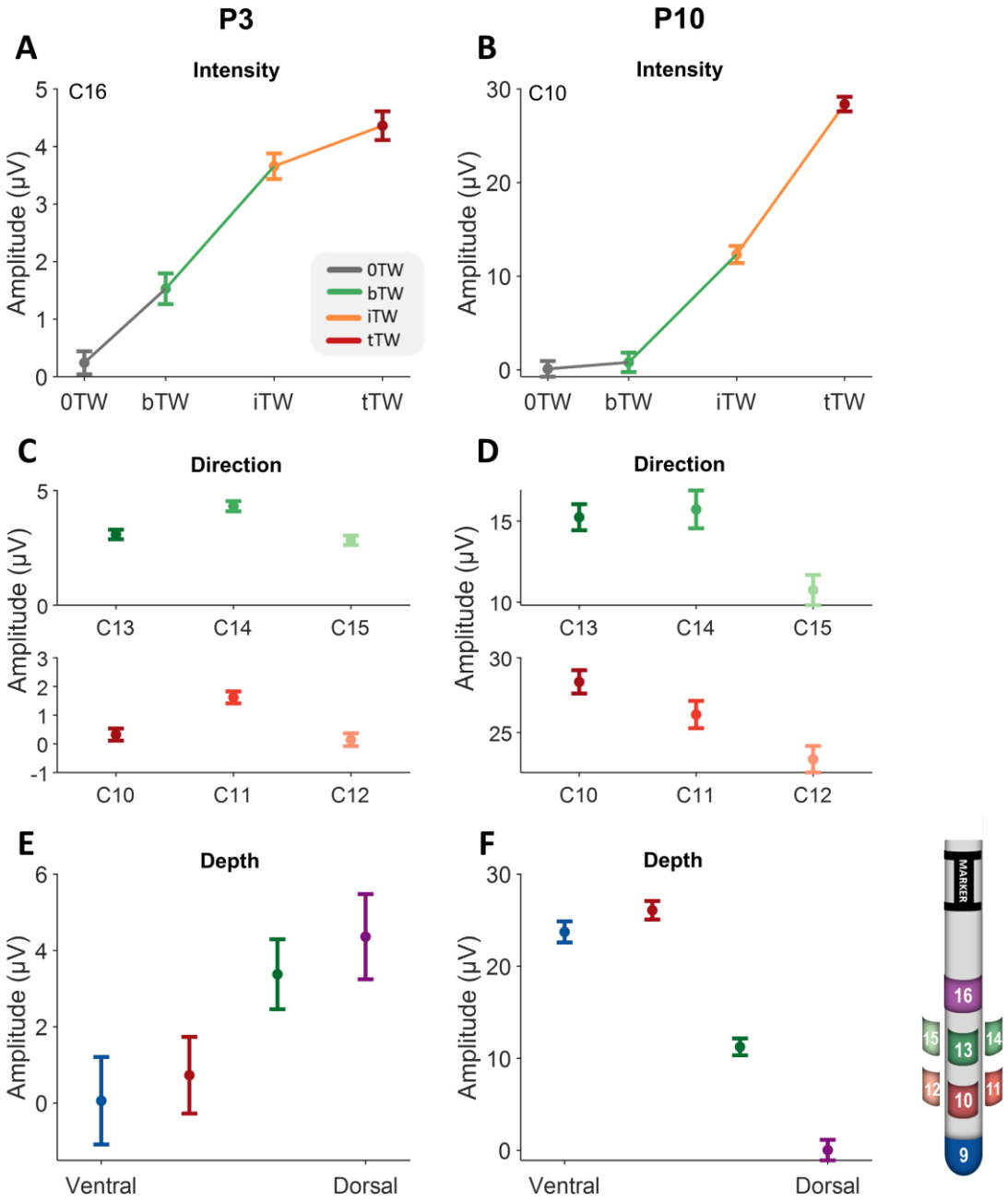

Left panels show the effect of DBS intensity (A), directionality (C) and depth (E) on P3 amplitude. Right panels show the effect of stimulation intensity (B), directionality (D) and depth (F) of P10 amplitude. The dots show the mean peak amplitude (P3 or P10) calculated across all epochs (n = 400), the error bars show the 95% confidence interval (CI). Colors for panels B, C, E and F indicate the EP recorded from a specific DBS-contact as shown on the right side. Different colors in panels A and B indicate the different stimulation intensities. Different colors in panels C-F indicate the different DBS-contact where the response is recorded from, as shown on the right bottom side.

Figure 4: P3 and P10 amplitudes are correlated with the distance to the STN and SNr respectively

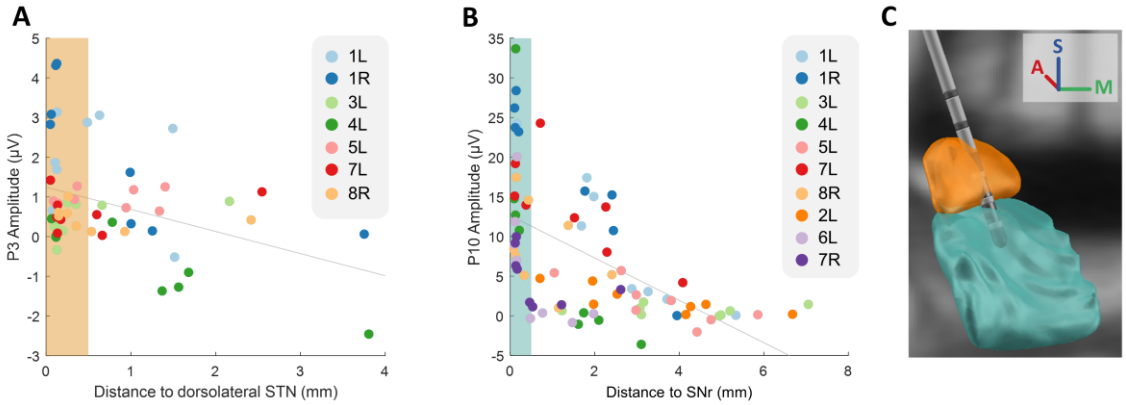

A) Relationship between the distance of each contact to the dorsolateral STN and the P3 amplitude recorded on that contact in seven hemispheres (n = 56). B) Relationship between the distance from each contact to their closest voxel of SNr and the P10 amplitude recorded on that contact in ten hemispheres (n = 80). The colors indicate the eight DBS-contacts of the same hemisphere. When the distance was smaller than 0.5 mm, the DBS-contact was determined as 'within' either dorsolateral STN (orange rectangle) or SNr (blue rectangle). C) Example of one lead implanted in STN (subject 4, left hemisphere), where the four dorsal DBS-contacts are positioned within STN, while the four ventral DBS-contacts are positioned within SNr (S: superior, M: medial, A: anterior).